Journal of Engineering and Sustainable Development
Vol. 30, No. 01, January 2026
https://jeasd.uomustansiriyah.edu.iq/index.php/jeasd
ISSN 2520-0917
Research Article
https://doi.org/10.31272/jeasd.2833

A Compact Ultra-Wideband Antenna Design for Satellite Communication Systems

Mohaimen Q. Algburi[1*], Ayman N. Muhi[1], Mustafa Ghanim[1], Nor Shahida Mohd Shah[2]

[1]College of Communication Engineering, University of Technology- Iraq, Baghdad, Iraq
[2]Faculty of Electrical and Electronic Engineering, Universiti Tun Hussein Onn Malaysia, Parit Raja 86400, Johor, Malaysia

[*]Email: corresponding_mohaimen.q.khalaf@uotechnology.edu.iq

Article Info

Received 09/07/2024
Revised 11/12/2025
Accepted 13/12/2025

Abstract

This paper presents a small-sized multilayer ultra-wideband (UWB) patch antenna for satellite communication applications in the X band, Ku band, and K band. The antenna consists of two stacked rectangular patches on the ground plane driven by H-shaped slots with miniaturized dimensions of 40 × 40 × 5.51 mm^3. The multilayer structure utilizes RT/Duroid®5880 and FR4 substrates, and simulation results show that the operational bandwidth is 15 GHz (8-23 GHz) with a reflection coefficient less than -10 dB. The proposed design exhibits stable omnidirectional radiation patterns, a peak gain of 8.3 dB, and an excellent VSWR across the entire operating band. The comparison of the proposed antenna against existing literature shows that the proposed antenna has a lot of benefits, as it achieves size reduction while maintaining broader bandwidth and higher gain than comparable designs. This antenna has a compact structure, coupled with high impedance matching and radiation properties, which makes this antenna convenient for the current generation of satellite communication systems that need miniaturized broadband components.

Keywords: Computer simulation technology, Double H-slot, Microstrip antenna, Ultra-wideband, Satellite applications

1. Introduction

Nowadays, the increasing demand for high-speed wireless communication and the proliferation of Internet of Things (IoT) devices have propelled researchers to explore novel antenna designs capable of supporting ultra-wideband (UWB) applications efficiently. UWB technology has been recognized for huge data rates of more than 100 Mbps and high efficiency compared with other wireless communication. Many studies have focused on the development and optimization of broadband antennas, driven by significant advances in UWB communication technologies over the past decade [1]. These studies have focused not only on improving bandwidth capabilities but also on enhancing antenna performance in terms of gain, efficiency, and radiation patterns. As a result, broadband antennas have garnered immense attention in academic and industrial research communities, shaping the future of wireless communication systems. UWB technology was first used in military applications, but after the Federal Communications Commission (FCC) approved it in 2002, it has been used in a variety of applications. This commission has determined the transmission power limits and the frequency bands allocated to various UWB applications. Any electromagnetic spectrum, technology, system, or signal with a bandwidth exceeding 0.5 GHz or more than 20% of the center frequency is referred to as ultra-wideband (UWB) [2]. The applications of ultra-wide antennas in this decade cover a variety of electronic platforms and Internet of Things (IoT) peripherals, due to their wide range and ease of integration with different communication systems. UWB antennas are important in wireless communication systems, especially in data exchange, tracking, sensing, monitoring, healthcare, and location identification. However, both applications have certain demands on the UWB antenna since the antenna design should be adjusted to the radiation properties that are determined by the respective communication system [3], [4].

During the past years, there has been a great deal of research work on the design and improvement of broadband antennas because of their favorable characteristics, such as high immunity to noise, low power consumption, the capability to penetrate different materials, enhanced resistance to multipath fading, and the ability to support high-data-rate wireless transmission over wide bandwidths. Despite these strengths, several challenges remain. These include increased implementation costs, slower adoption, longer signal acquisition times, challenges in integrating UWB systems, and potential interference or overlap with other radio systems [5],

[6]. Moreover, despite the large number of compact UWB antenna designs proposed, not all are suitable for satellite communication. This weakness is mainly due to design trade-offs. For example, antennas for the X, Ku, and K bands must be compact; however, to achieve good performance, a suitable matching network may be required, which can increase the overall size of the antenna system. In addition, the diameter and height of UWB antennas are directly proportional to their peak bandwidth. Therefore, the size reduction of UWB antennas has to face some fundamental limitations of reducing the impedance bandwidth with the diameter of the antennas. Thus, it might be difficult to design small UWB antennas with a wide bandwidth, sufficient radiation efficiency, and reliable resistance matching across the range of frequencies. A few instances of these difficulties are the antenna's performance being impacted by size restrictions and the difficulty of incorporating several UWB bands within the same antenna design. To overcome these obstacles and keep the antenna design small, new approaches such as sophisticated matching networks, multilayer patches, frequency-selective surfaces, and metamaterials may be used [7]. An extensive operating bandwidth is essential for UWB antenna systems. However, because UWB antennas must meet stringent specifications, including small size, broadside emission patterns, low VSWR, good impedance matching, and large bandwidth, designing a UWB antenna can be challenging [8]. Furthermore, high-gain antennas with excellent directivity are required for several wireless communication applications, including positioning systems, radar, location tracking, and monitoring [9], [10].

The design of UWB antennas affects the overall performance of UWB systems [11]-[19]. However, the radiation pattern utilized in wireless systems influences UWB antenna design, and these antennas could be categorized according to this pattern. There are two such categories: omnidirectional UWB antennas enable effective communication between a receiver and a transmitter in multiple directions due to their omnidirectional radiation pattern. These antennas are appropriate for mobile devices and indoor wireless communication. The second category is directional UWB antennas. In these antennas, the high-power signals are restricted to being received or transmitted in specific directions. The antenna performs better and causes less interference due to its directional radiation pattern. An example of a co-planar ultra-wideband antenna with a directive radiation pattern is the Vivaldi antenna [20]. UWB antennas have a variety of applications, for example, satellite communications systems, ground penetrating radars, flexible electronic devices, and imaging systems [21]-[24], and due to their small size, ease of integration, and rapid technological development, UWB antennas have become more popular in a wide range of other applications. Antennas with a UWB spectrum with filtering properties are urgently needed not only to mitigate interference but also to remove the requirement for additional notch filters [25]. Several techniques are used in the design of wideband antennas to achieve a wide operating range. The use of isolated slots embedded within the radiator, defective ground structures, and various patch configurations, such as E-, T-, U-, and H-shaped slots, complex structures, and fractal structures, to improve antenna parameters has been reported [26]-[31]. Agarwal et al. [15] introduced a 4×4 MIMO array antenna operating in the frequency range 3.3-16.5 GHz. The antenna is fed via the coplanar waveguide (CPW) method. However, the average gain did not exceed 3.5 dBi. Sharifi et al. [16] introduced the beam-steering array antenna with a gain of 9.5 dBi and a return loss of S_{11} < -14 dB. This antenna operates over the frequency band from 20.5 GHz to 30 GHz. Sarkar et al. [17] presented a rectangular air-gap antenna with distorted ground structures in the X- and Ku-band ranges. The antenna achieved a bandwidth of 58.72% (8.3-15.2) GHz. However, there are difficulties associated with antenna size, beamforming, and design complexity. Baladi et al [18] presented a reconfigurable antenna based on the unit cell in the frequency ranges of (10.8-11.8) GHz and (14-15.4) GHz within the Ku band. The unit cell consists of two circular loops, and to achieve beam controllability, each loop is loaded with four variable diodes. However, the antenna achieved a poor bandwidth of 4.3%. In other designs presented by Wu et al. [14], Agarwal et al. [15], and Chung et al. [32], the antennas fail to achieve good gain across the operating range due to their small frame size. As a result, ultra-wideband antennas have poor directivity. Anim et al. [22] developed a wide-band antenna array for X-band applications. The antenna consisted of several layers: three copper layers and two insulating substrates. The antenna has a large size of 371×276 mm². To separate the layers, Rohacell foam material was utilized. The results show that the maximum bandwidth was 12.4% (9.01-10.20) GHz. Din et al. [24] reported a semi-circular UWB monopole antenna. To improve the antenna's bandwidth, the ground plane was distorted, and a 6×6 metal reflector Frequency-Selective Surface (FSS) was inserted below the antenna to enhance the gain. However, the antenna's 62.5×63×25 mm3 dimensions and fabrication difficulty make it unsuitable for many applications.

In this work, a simple UWB multilayer patch antenna for satellite communication applications is presented. The proposed antenna is designed, simulated, and tested using CST and HFSS packages. The operating frequency range is 10 GHz to 25 GHz, and the layers comprise RT/Duroid®5880 and FR4 with overall dimensions of 40×40×5.51 mm^3. We used an H-shaped probe, as one of the previously mentioned methods, to achieve UWB. The antenna consists of four substrates: the first three are of the same type (FR4) and are connected to a copper ground plane. The antenna achieves UWB functionality by using a dual H-shaped feed slot and two optimized design patches, coupled to each other. Compared with traditional microstrip antennas, the proposed antenna achieved return loss < -10dB, a fractional bandwidth of 15 GHz (100%), and a maximum gain of 8.3 dB.

The article is organized as follows: Section 2 describes the structure of the proposed antenna geometry in detail; the antenna comprises multiple layers. The parametric study was presented in Section 3, which explains the stages of antenna design to achieve optimal results. Subsequently, the antenna simulation results are presented and discussed in detail in Section 4, and the conclusions are presented in Section 5.

2. Method of the Research

2.1 Antenna Design Detail

The proposed antenna operates in the (X, Ku, and K bands). The required frequency was calculated based on the calculations:

$$f_{TM} = \frac{c}{2\pi\sqrt{\varepsilon_r}}\sqrt{\left(\frac{m\pi}{Wp}\right)^2 + \left(\frac{m\pi}{Lp}\right)^2} \quad (1)$$

Where Lp and Wp represent the effective length and width calculated according to [14]. At the ground plane, two H-shaped feeding slots were etched to enhance the antenna parameters. The structural dimensions of the slot meet the following requirements:

$$Lg_1 + Lg_2 + Lg_3 \approx \lambda g \quad (2)$$

Where it is possible to adjust the values $Lg_1 \approx \frac{\lambda g}{2}$, $Lg_3 \approx \frac{\lambda g}{4} = Lg_2$, to improve the impedance match. Means that the overall effective length of the slot, which is the sum of the three segments Lg_1, Lg_2, and Lg_3, must be about equal to the guided wavelength λg. This condition is necessary to make the slot a resonant path, which contributes to the enhancement of impedance matching at the required operating frequency.

In the first phase of our study, we adopted the configuration proposed by Li et al. [29], which features a multilayer architecture including an H-shaped feed line and a two-patch design. Simulation of this configuration in an HFSS system demonstrated an operating bandwidth of 12–18.25 GHz, corresponding to a 41.3% subband with a VSWR < 2. We then optimized the design by introducing additional methods to expand the operational bandwidth and broaden the range of possible applications. To achieve this, an H-shaped probe was added, and the radiating-patch geometry was changed to square and rectangular. These modifications reduced the structure and ultimately decreased the overall antenna size. The proposed antenna is shown in Fig. 1. The antenna structure comprises four parts. The first part contains a square patch. The patch is printed after modification to obtain the optimal design on the upper surface of the first part, using a Roger RT/Droid 5880 (ε_r= 2.2) dielectric substrate with a thickness of 0.575mm. The second part contains a patch whose dimensions have been adjusted to increase impedance matching, with an FR4 layer (ε_r= 4.4) dielectric substrate. In the third part, a double-H aperture coupling printed on a ground plane is used, with aperture dimensions optimized to achieve the maximum bandwidth of the proposed antenna. In the last part, the proposed antenna is fed through a microstrip line with a 50 Ω SMA connector. The dimensions of the proposed antenna are shown in Table 1.

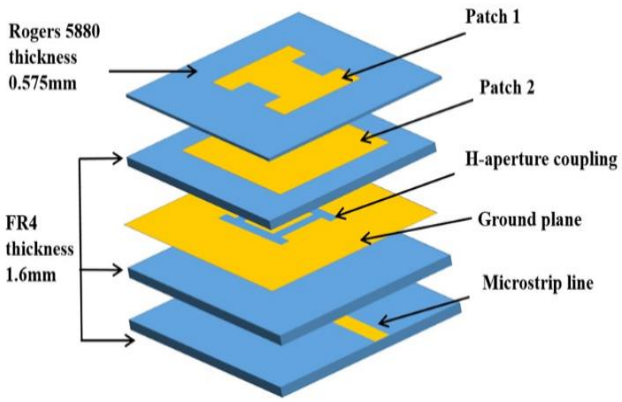

(a)

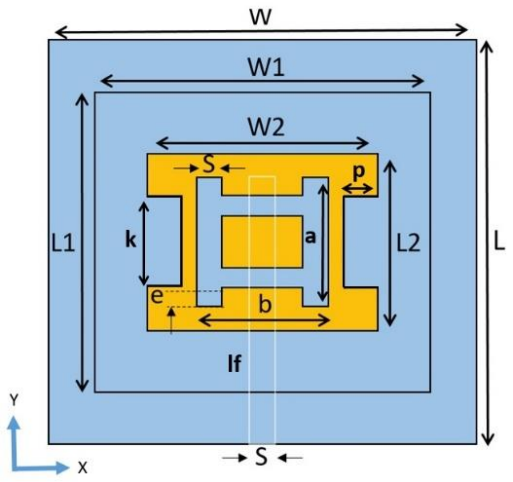

(b)

Figure 1. The proposed antenna structure: (a) 3D antenna, (b) top view

Table 1. Dimension of the multilayer antenna.

Parameter	Value (mm)
W (width ground, substrate)	40
L (length ground, substrate)	40
W1 (width patch 2)	30
L1 (length patch 2)	27
W2 (width patch 1)	20
L2 (length patch 1)	17
lf (length of feed)	26
a	13
b	13
k	9
p	2.5
e	1
S	2

2.2. The Parametric Study

In this section, the parametric study shows how the three stages of designing the proposed antenna were performed across different frequencies, with respect to antenna gain and return loss (S11), which indicates the extent to which the radio signal is reflected by the antenna rather than transmitted. A lower S_{11} score is better. As a result, a more negative S_{11} value in decibels means less reflection. Usually, the more negative the number, the better the antenna is matched to the feed line that connects it to the source of the signal. A better match results in more power radiated by the antenna than reflected. In general, the lower and more negative the S11 value, the better the antenna performs at transmitting the signal rather than reflecting it. Fig. 2 shows the stages of configuring the proposed antenna, and Fig. 3 shows the effect of layers on the performance of the proposed multi-layer antenna, specifically how it affects the gain, which is a measure of the antenna's efficiency, and the scattering parameter (S_{11}), which is a measure of reflected power. The x-axis is a frequency in GHz, and the y-axis is return loss (S_{11}) in decibels. The analysis of the results indicates that the antenna configuration stages (Ant 1) exhibit dual-band performance at 14.5 GHz and 21.5 GHz, with operating ranges of 2.3 GHz and 1.4 GHz, respectively. The antenna also achieved a gain of 7.8 dB at 14.5 GHz and 8.4 dB at 21.5 GHz. The effect of introducing layers (Ant 2 and Ant 3) on the performance of the proposed antenna was found to be significant. When the (Ant 2) layer was introduced, the two frequency bands were cancelled, and the proposed antenna became ultra-wideband (UWB). However, there is a need to improve impedance matching and return loss. As a result, the (Ant 3) layer was introduced and modified to obtain the optimal design. In addition, the (Ant 3) layer improved the performance of the proposed antenna by enhancing impedance matching, return loss, and operating range, as shown in Fig. 3.

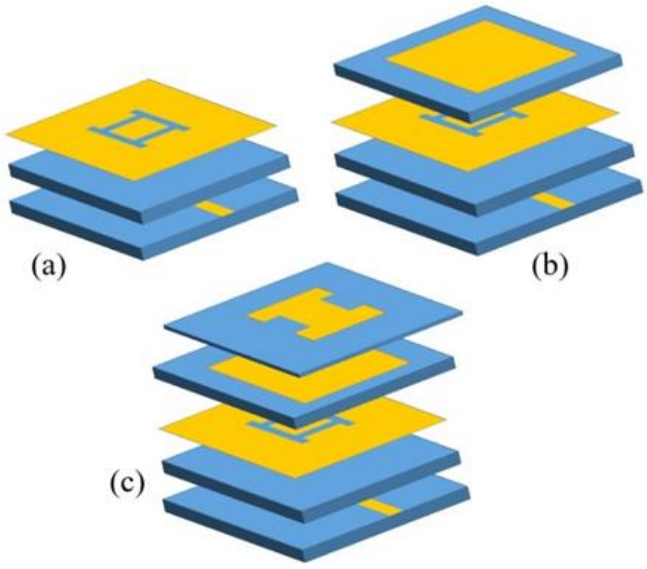

Figure 2. Stages of configuring the proposed antenna: (a) Ant1, (b) Ant2, (c) Ant3

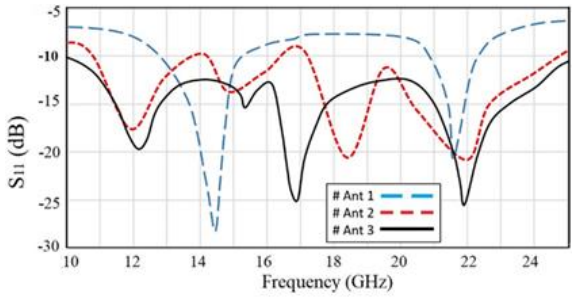

(a)

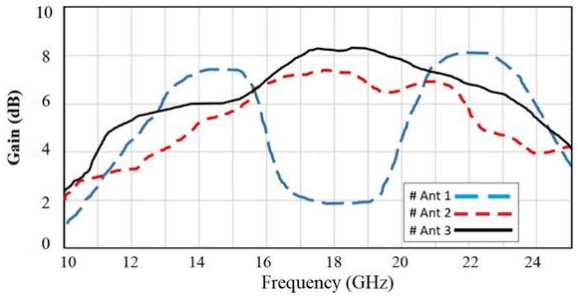

(b)

Figure 3. Simulated (a) return loss and (b) gain value for each stage of the proposed antenna configuration

3. Results and Discussion

The simulation gives us three resonance modes centered around the frequencies 12 GHz, 17 GHz, and 22 GHz with a S_{11} < -10 dB reflection coefficient from 10 GHz to 25 GHz. This bandwidth covers applications in the X-, Ku-, and K-bands, namely radar and satellite communication systems.

The reflection coefficient of the proposed antenna is shown in Fig. 4 and was analyzed using both CST MW version 19 and HFSS version 17 to ensure the accuracy of the results. The multilayer design significantly enhances the antenna's bandwidth and enables effective operation across a broader frequency range. In addition, the proposed antenna operates between 10 GHz and 25 GHz, with a reflection coefficient S11 < -10 dB due to excellent impedance matching and sound isolation between the antenna elements. We observe three modes of resonance. The presence of these resonances is explained by the presence of the multilayer patch. Fig. 5 shows the simulated VSWR.

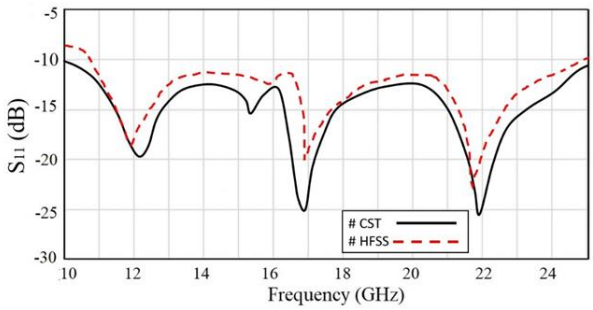

Figure 4. Analysis S_{11} of the proposed antenna

VSWR "is an indication of the mismatch ratio between the antenna and the feed line to which it is connected." It is used as an efficiency measure for all radio-frequency transmission systems, including transmission lines. A VSWR value between 1 and 2 is suitable for most antenna applications, indicating a good match. Fig. 5 shows the simulated VSWR.

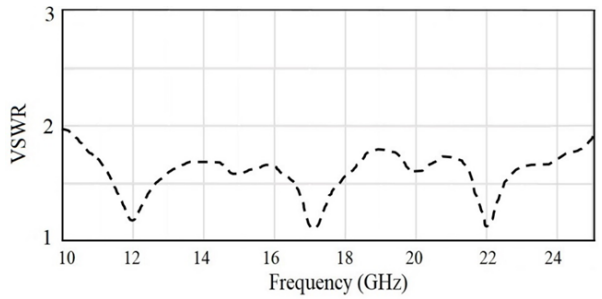

Figure 5. Analysis of the VSWR of the proposed antenna

Fig. 6 presents the radiation patterns in the H- and E-planes for the three resonance frequencies, 12 GHz, 17 GHz, and 22 GHz. We note that the radiation patterns are almost omnidirectional, which is desirable in satellite applications.

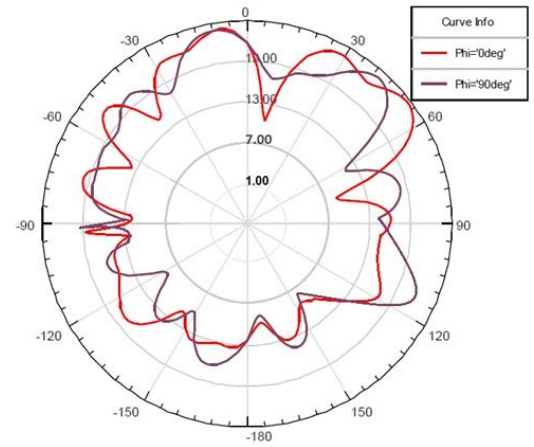

(a)

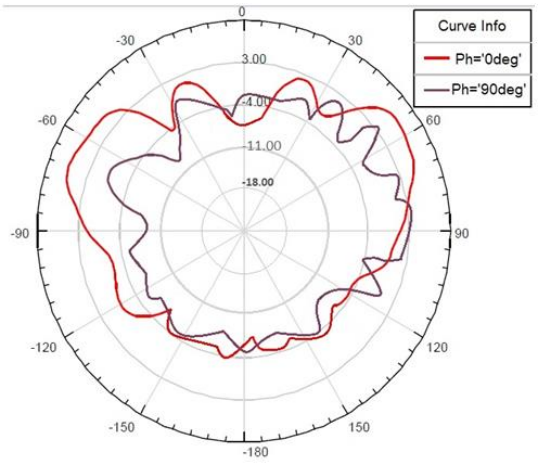

(b)

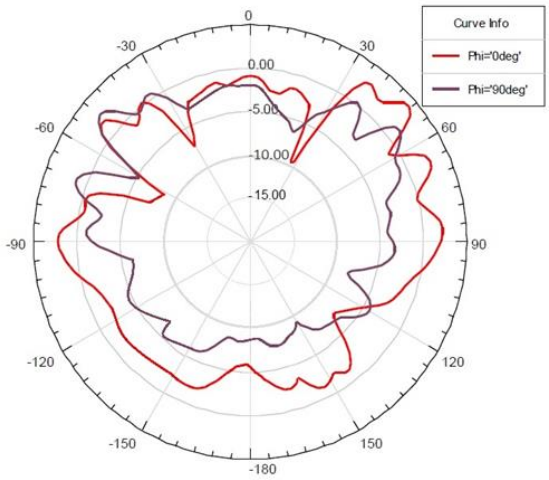

(c)

Figure 6. H plane and E plane radiation patterns: (a) 12 GHz, (b) 17 GHz and (c) 22 GHz

Fig. 6 shows the 2D radiation pattern for the three frequency modes. It is found that at 12 GHz, the pattern is omnidirectional with three major lobes. This is attributed to the current distribution, as fewer surface waves are present due to the isolation between the antenna components. Isolation is enhanced by minimizing the propagation of surface waves on the antenna and its surroundings, thereby reducing interaction with neighboring objects. This results in improved separation between antenna elements, leading to higher signal quality and increased radiation efficiency. The confinement of currents within each segment enhances electromagnetic wave radiation, thereby improving the antenna's effectiveness in converting electrical power into electromagnetic waves. For the other two frequencies, the radiation pattern is nearly omnidirectional. Fig. 7 shows the current distributions of the proposed antenna, where currents are concentrated in the lower part of the antenna structure and then dispersed by the H-slot and the good isolation between the antenna elements, thereby maintaining the antenna's performance without deterioration.

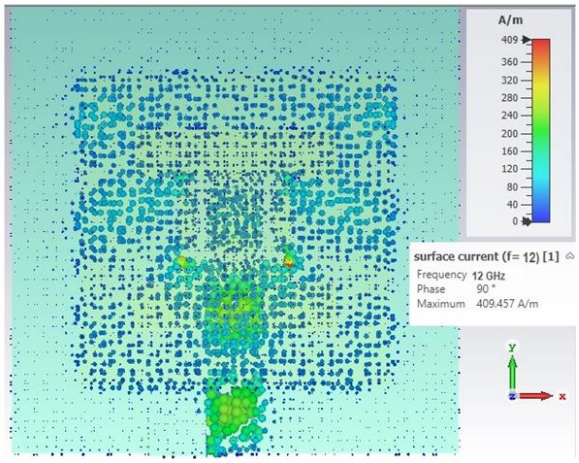

(a)

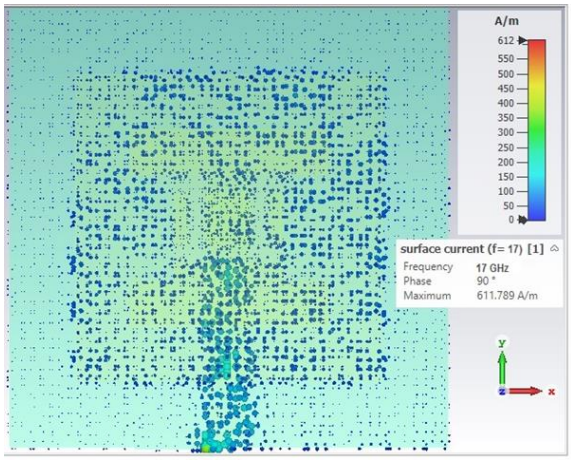

(b)

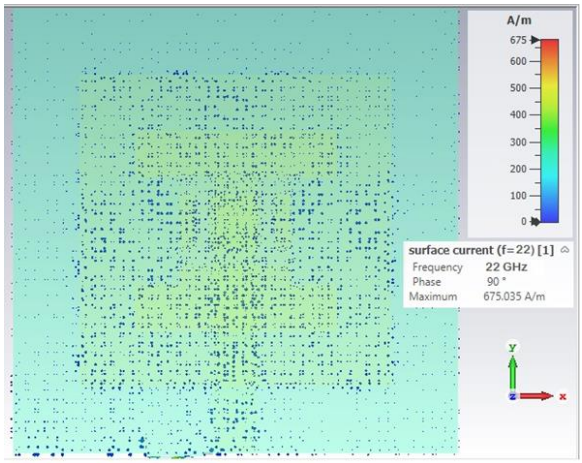

(c)

Figure 7. Analysis of current distribution: (a) 12 GHz, (b) 17 GHz, and (c) 22 GHz

The performance of the proposed antenna, in terms of operating range, substrate size, gain, and design complexity, is compared with results reported in the recent literature. It was noted that the proposed antenna has a wide operating range covering between 10 GHz and 25 GHz with good gain and ease of design, as shown in Table 2. Accordingly, the proposed antenna is suitable for modern communication applications.

4. Conclusions

The paper introduces a compact ultra-wideband patch antenna for satellite communication systems. The antenna has three significant contributions; (1) the antenna has a miniaturized design: 40 × 40 × 5.51 mm^3 with four-layer substrate structure made of RT/Duroid 5880 and FR4 materials, (2) the antenna is ultra-wideband with 100% fractional bandwidth of 15 GHz, (3) the antenna has stable omnidirectional radiation patterns with a peak gain of 8.3 dB and an excellent VSWR.

The originality of the proposed design lies in the dual H-shaped slot feeding mechanism and an optimal stacked patch configuration, which enable compact size and ultra-wideband performance simultaneously. Compared with recent work, the antenna offers competitive performance, and its structure is simpler than that of other designs.

The main drawback of this work is the trade-off between compactness and gain, in which the miniaturized structure limits the gain to the highest possible 8.3 dB. Additionally, the omnidirectional radiation pattern, although beneficial for satellite communication links, limits the directional control of beam-steering applications.

Table 2. The Comparison of the proposed antenna with recently published work.

Ref.	Size $(mm)^2$	Material	Freq. range (GHz)	B.W (%)	gain (dBi)
[21]	20.5×13.9	polyimide	3–16.2	—	8.4
[22]	371×276	Taconic	2.75–16.05	141	5
[23]	80×80	FR-4	8.3–15.2	58.7	5–6.5
[24]	62.5×63	FR-4	12.2–27.1	75.8	5.6
[14]	60×60	FR-4	14–15.4	4.3	16.61
[15]	55×55	FR-4	15.19–16.02	5.31	3.5
[17]	60×60	duroid	3.6-19.08	136.51	3
[18]	60×60	RO4003	9–10.2	12.4	28
[19]	20×30	RO4003C	12–14.13	17	14.2
[32]	30×13	DiClad 880	3–11	—	8.3
This work	40×40	RT/5880	10–25	100	8.3

Future work will focus on three directions: first, electromagnetic bandgap (EBG) structures will be incorporated into the ground plane to prevent the propagation of surface waves and to enhance gain without increasing the antenna size. Second, exploration of metamaterial loading to enhance impedance matching across a wide range of frequencies, potentially extending to additional satellite bands. Third, the reconfigurable versions are developed using PIN diodes or varactor diodes, which enable frequency tuning and adaptive bandwidth control for multi-mission satellite platforms.

The performance features demonstrated, small size, consistent radiation patterns, and simplicity have made this antenna a viable option for the modern satellite communication system seeking miniaturized components of broadband performance with consistent operation in the X, Ku, and K bands.

Acknowledgements

The authors are grateful for the support for this research from the Communication Engineering College, University of Technology, Iraq. As a group of lecturers working in this department, we extend our gratitude to this college and our university.

Conflict of interest

The authors declare no conflict of interest.

Author Contribution Statement

Mohaimen Q. Algburi proposed the research problem, developed the idea, and outlined the key concepts. Ayman N. Muhi, Mustafa Ghanim, and Nor Shahida Mohd Shah contributed to the planning, interpretation of the results, and follow-up on the work. Mohaimen Q. Algburi processed the experimental data, performed analyses using HFSS and CST, and drafted the manuscript. All authors discussed the results and contributed to the final manuscript.

References

[1] S. Liu et al., "A Dual-Band Shared Aperture Antenna Array in Ku/Ka-Bands for Beam Scanning Applications," IEEE Access, vol. 7, pp. 78794–78802, Jan. 2019, https://doi.org/10.1109/access.2019.2922647.

[2] Federal Communications Commission (FCC). Revision of Part 15 of The Commission's Rules Regarding Ultra-Wideband Transmission Systems. In : First Report and Order, ET Docket. Washington, DC, USA; 2002. p. 98–153.

[3] H. Q. Al-Gburi, M. Algburi, and H. Al-Saedi, "Compact Antenna Design for RFID and IoT Applications," 2022 *2nd International Conference on Computing and Machine Intelligence (ICMI)*, pp. 1–4, Apr. 2022, https://doi.org/10.1109/icmi55296.2022.9873727

[4] O. P. Kumar, P. Kumar, T. Ali, P. Kumar, and S. Vincent, "Ultrawideband Antennas: Growth and Evolution," *Micromachines*, vol. 13, no. 1, p. 60, Dec. 2021, https://doi.org/10.3390/mi13010060

[5] M. Damou, Y. Benallou, B. Mansouri, K. Nouri, M. Chetioui, and A. Boudkhil, "SIW/HMSIW Bandpass Filters for Ka Frequency Band Serving Wireless Applications," *International Journal of Electronics and Telecommunications*, vol. 67, no.3. pp. 355–361, Jul. 2021,

[6] S. K. Hassan, A. H. Sallomi, and M. H. Wali, "Design of A Dual-Band Rejection Planar Ultra-Wideband (UWB) Antenna," *Journal of Engineering and Sustainable Development*, vol. 26, no. 4, pp. 30–35, Jul. 2022, https://jeasd.uomustansiriyah.edu.iq/index.php/jeasd/article/view/1572

[7] S. Jayant et al., "Decoupling Methods in Planar Ultra-Wideband Multiple-Input-Multiple-Output Antennas: A Review of the Design, State-of-the-Art, and Research Challenges," *Electronics*, vol. 12, no. 18, p. 3813, Sep. 2023, https://doi.org/10.3390/electronics12183813.

[8] B. Li, Y. Wang, J. Zhao, and J. Shi, "Ultra-Wideband Antennas for Wireless Capsule Endoscope System: A Review," *IEEE Open Journal of Antennas and Propagation*, vol. 5, no. 2, pp. 241–255, Apr. 2024, https://doi.org/10.1109/ojap.2024.3355217

[9] R. De Marco, E. Arnieri, F. Greco, A. Bordbar, G. Amendola, and L. Boccia, "Low-Profile Dual-Band Dual-Polarized Transmitarray Antenna Based on Multilayer Frequency Selective Surfaces," *IEEE Transactions on Antennas and Propagation*, vol. 71, no. 9, pp. 7354–7362, Sep. 2023, https://doi.org/10.1109/tap.2023.3296257

[10] A. K. Nghaimesh and A. K. Jassim, "Triple-Band Circular Patch Microstrip Antenna For Wireless Communication," *Journal of Engineering and Sustainable Development*, vol. 28, no. 1, pp. 64–74, Jan. 2024, https://doi.org/10.31272/jeasd.28.1.5

[11] R. B. Nassir and A. K. Jassim, "Design of Mimo Antenna For Wireless Communication Applications," *Journal of Engineering and Sustainable Development*, vol. 26, no. 4, pp. 36–43, Jul. 2022, https://doi.org/10.31272/jeasd.26.4.4

[12] M. Al-Tamimi and R. H. Thaher, "Design Of New Compound Reconfigurable Microstrip Antenna For C And Ku Bands Applications," *Journal of Engineering and Sustainable Development*, vol. 27, no. 2, pp. 196–203, Mar. 2023, https://doi.org/10.31272/jeasd.27.2.4

[13] H. Al-Saedi et al., "An Integrated Circularly Polarized Transmitter Active Phased-Array Antenna for Emerging Ka-Band Satellite Mobile Terminals," *IEEE Transactions on Antennas and Propagation*, vol. 67, no. 8, pp. 5344–5352, Aug. 2019, https://doi.org/10.1109/tap.2019.2913745

[14] W. Wu, B. Yuan, and A. Wu, "A Quad-Element UWB-MIMO Antenna with Band-Notch and Reduced Mutual Coupling Based on EBG Structures," *International Journal of Antennas and Propagation*, vol. 2018, pp. 1–10, 2018, https://doi.org/10.1155/2018/8490740

[15] S. Agarwal, U. Rafique, R. Ullah, S. Ullah, S. Khan, and M. Donelli, "Double Overt-Leaf Shaped CPW-Fed Four Port UWB MIMO Antenna," *Electronics*, vol. 10, no. 24, p. 3140, Dec. 2021, https://doi.org/10.3390/electronics10243140

[16] G. Sharifi, Y. Zehforoosh, T. Sedghi, and M. Takrimi, "A high gain pattern stabilized array antenna fed by modified Butler matrix for 5G applications," *AEU - International Journal of Electronics and Communications*, vol. 122, p. 153237, Jul. 2020, https://doi.org/10.1016/j.aeue.2020.153237

[17] T. Sarkar, A. Ghosh, L. L. K. Singh, S. Chattopadhyay, and C.-Y.-D. Sim, "DGS-Integrated Air-Loaded Wideband Microstrip Antenna for X- and Ku-Band," *IEEE Antennas and Wireless Propagation Letters*, vol. 19, no. 1, pp. 114–118, Jan. 2020, https://doi.org/10.1109/lawp.2019.2955111

[18] E. Baladi, M. Y. Xu, N. Faria, J. Nicholls, and S. V. Hum, "Dual-Band Circularly Polarized Fully Reconfigurable Reflectarray Antenna for Satellite Applications in the Ku-Band," *IEEE Transactions on Antennas and Propagation*, vol. 69, no. 12, pp. 8387–8396, Dec. 2021, https://doi.org/10.1109/tap.2021.3090577

[19] I. A. Zubir et al., "A Low-Profile Hybrid Multi-Permittivity Dielectric Resonator Antenna With Perforated Structure for Ku and K Band Applications," *IEEE Access*, vol. 8, pp. 151219–151228, 2020, https://doi.org/10.1109/access.2020.3016432

[20] J. Ren, H. Fan, Q. Tang, Z. Yu, Y. Xiao, and X. Zhou, "An Ultra-Wideband Vivaldi Antenna System for Long-Distance Electromagnetic Detection," *Applied Sciences*, vol. 12, no. 1, p. 528, Jan. 2022, https://doi.org/10.3390/app12010528

[21] Q. Zou and S. Jiang, "A compact flexible fractal ultra-wideband antenna with band notch characteristic," *Microwave and Optical Technology Letters*, vol. 63, no. 3, pp. 895–901, Sep. 2020, https://doi.org/10.1002/mop.32678

[22] K. Anim, P. Danuor, S.-O. Park, and Y.-B. Jung, "High-Efficiency Broadband Planar Array Antenna with Suspended Microstrip Slab for X-Band SAR Onboard Small Satellites," *Sensors*, vol. 22, no. 1, p. 252, Dec. 2021, https://doi.org/10.3390/s22010252

[23] Y. I. Abdulkarim et al., "A Low-Profile Antenna Based on Single-Layer Metasurface for Ku-Band Applications," *International Journal of Antennas and Propagation*, vol. 2020, pp. 1–8, Dec. 2020, https://doi.org/10.1155/2020/8813951

[24] I. U. Din et al., "Improvement in the Gain of UWB Antenna for GPR Applications by Using Frequency-Selective Surface," *International*

Journal of Antennas and Propagation, vol. 2022, no.1. pp. 1–12, Oct. 2022, https://doi.org/10.1155/2022/2002552

[25] M. Zhang et al., "An Ultra-Wideband Integrated Filtering Antenna with Improved Band-Edge Selectivity Using Multimode Resonator," *Electronics*, vol. 12, no. 15, p. 3264, Jul. 2023, https://doi.org/10.3390/electronics12153264

[26] M. A. Gburi and M. Ilyas, "A Novel Design Reconfigurable Antenna Based on the Metamaterial for Wearable Applications," *Journal of Physics: Conference Series*, vol. 1973, no. 1, p. 012042, Aug. 2021, https://doi.org/10.1088/1742-6596/1973/1/012042

[27] K. Srivastava, S. Singh, A. K. Singh, and R. Singh, "Dual Band Integrated Wideband Multi Resonating Patch Antenna for C–Band and Ku–Band Applications," *International Journal of Electronics and Telecommunications*, pp. 347–352, Jan. 2019.

[28] M. Y. Muhsin, A. J. Salim, and J. K. Ali, "Compact MIMO Antenna Designs Based On Hybrid Fractal Geometry for 5 G Smartphone Applications," *Progress In Electromagnetics Research C*, vol. 118, pp. 247–262, 2022, https://doi.org/10.2528/pierc22012808

[29] R. Li et al., "Design of Wideband High-Gain Patch Antenna Array for High-Temperature Applications," *Sensors*, vol. 23, no. 8, p. 3821, Apr. 2023, https://doi.org/10.3390/s23083821

[30] K. C. Paul and A. Ahmed, "E-shaped Aperture Coupled Microstrip Patch Array Antenna for High Speed Downlink Applications in Small Satellites," *International Journal of Electronics and Telecommunications*, pp. 47–56, Dec. 2021, https://doi.org/10.24425/ijet.2022.139847

[31] A. J. Salim, J. K. Mohammed, H. Al-Saedi, and J. K. Ali, "A Proximity-fed Multi-band Printed Antenna for Wireless Communication Applications," *Progress In Electromagnetics Research C*, vol. 145, pp. 153–165, 2024, https://doi.org/10.2528/pierc23122503

[32] M.-A. Chung, K.-C. Tseng, and I.-P. Meiy, "Antennas in the Internet of Vehicles: Application for X Band and Ku Band in Low-Earth-Orbiting Satellites," *Vehicles*, vol. 5, no. 1, pp. 55–74, Jan. 2023, https://doi.org/10.3390/vehicles5010004